Supplementary material

Extraction of ofloxacin from water using hydrophobic eutectic solvents

Mahtab Moradi[1,2], Ana M. Ferreira[1*], Catarina M. S. S. Neves[1], Samane Zarei Mahmoudabadi[2], Gholamreza Pazuki[2*], and João A.P. Coutinho[1]

[1]CICECO – Aveiro Institute of Materials, Department of Chemistry, University of Aveiro (UA), 3810-193 Aveiro, Portugal.

[2]Department of Chemical Engineering, Amirkabir University of Technology (Tehran Polytechnic), 1591634311 Tehran, Iran.

Corresponding authors: Ana M. Ferreira and Gholamreza Pazuki

*E-mails: ana.conceicao@ua.pt and ghpazuki@aut.ac.ir

Tables

Table S1. Summary of some recent studies employing HES-based LLE for extracting various pharmaceuticals from water-based samples.

Analytes	Sample matrix	HES (mol:mol)	Method	Recovery (%)	Key findings	Ref.
Oxytetracycline, Doxycycline, Tetracycline	Water	Thymol: Octanoic acid (1:1)	Dispersive LLME	74-113	Choline chloride: ethylene glycol HES was used as disperser solvent. Thymol: Octanoic acid HES was used as extraction solvent. The addition of beta-cyclodextrin (β-CD) to the extraction phase improved extraction efficiencies.	[1]
Levofloxacin, Ciprofloxacin	Spiked water	Thymol: Hexanoic acid (2:1)	LLME	94-110	Four HES were used as extraction solvent. The impact of the solution pH, of the phase transition behavior of the HES was studied.	[2]
Salicylic acid, Oxaprozin, Diclofenac, Ibuprofen	Water and Milk	Thymol: 1,1,3,3-tetramethylguanidine chloride (2:1)	Ultrasound-assisted Dispersive LLME	79–107	Three HES composed of guanidinium chloride and thymol, methyltrioctylammonium chloride and thymol, and choline chloride and thymol were used as extraction solvent.	[3]
Ofloxacin, Norfloxacin, Ciprofloxacin, Enrofloxacin	Surface water	Thymol: Heptanoic acid (2:1)	LLME	84–113	The developed method based on in situ formation of twenty one HES (composed of thymol, menthol, and camphor and fatty acids) coupled with shaker-assisted LLME (in situ HES-SA-LLME) was validated.	[4]
Sulfamethoxazole, Sulfamethazine, Sulfapyridine	Urine	Vanillin: Menthol (1:1) Vanillin;Thymol (1:1)	LLME	91–93	Thymol and Vanillin were used as both media for Schiff bases formation and the precursor of HES.	[5]
Ketoprofen, Diclofenac	Urine	Menthol: Analytes	LLME	93-97	The procedure was applied based on in-situ HES formation and menthol used as extractant solvent.	[6]
Terbutaline, Clorprenaline, Tulobuterol, Clenbuterol, Salbutamol	Water	Tetra butyl ammonium chloride: Decanoic acid (1:3)	Dispersive LLME	56 - 91	Nine HES based on quaternary ammonium salts and fatty acids were prepared.	[7]
Ciprofloxacin	Water	Decanoic acid: Dodecanoic acid (2:1)	LLE	90	Ten HES based on quaternary ammonium salts, menthol and fatty acids were prepared.	[8]
Tetracycline, Oxytetracycline, Chlortetracycline	Water	Methyltrioctylammonium chloride: Nonanoic acid (1:2)	LLME	77- 87	Ten HES based on quaternary ammonium salts, fatty acids and fatty alcohol as extraction solvents were prepared.	[9]

Tetracycline, Doxycycline, Oxytetracycline	Water	Choline chloride: Thymol: Nonanoic acid (1:2:2)	Dispersive LLME	74–95	Four new thymol-based ternary HES were prepared. The ES hydrophobicity and its effect on the pH of water samples was studied.	[10]
Levofloxacin, Ciprofloxacin	Water	Tricaprylylmethylammonium chloride: 1-octanol (1:1)	LLME	94.8	Sixteen HES based on quaternary ammonium salts; fatty acids and fatty alcohol were prepared.	[11]
Sulfadiazine, Sulfamerazine, Sulfametoxydiazine, Sulfamethoxazole	Water	Choline chloride: o-cresol Choline chloride: m-cresol Choline chloride: p-cresol (1:2)	Dispersive LLME	80–93	The three HES showed commendable performance for extraction of sulfonamides compared to hydrophilic DESs.	[12]
Carbamazepine	Aqueous solution	Menthol: acetic acid (1:1)	Reactive LLE	> 90	The study used of various carboxylic acid based deep eutectic liquids (DEL) such as menthol: acetic acid / formic acid --Diethyl succinate and DEL were used as diluent and extractant.	[13]
Diclofenac	Aqueous solution	DL-menthol: Acetic acid (1:1)	Reactive LLE	47- 78	The designed HES enhanced the removal of diclofenac by more than 2.7 to 4.5 times compared to a conventional solvent. Diethyl succinate and HES were used as diluent and extractant.	[14]
Valsartan	Aqueous solution	L-menthol: (+)-Di-p-toluoyl-D-tartaric Acid (8:1)	LLE	91	Four hydrophobic DESs with five hydrophilic DESs were studied for enantioseparation of valsartan.	[15]

Table S2. Compound, CAS number, molecular weight (M_w), supplier, purity, and logarithm of the octanol-water partition coefficients (logK_{OW}).

Compound	**CAS number**	**M_w (g/mol)**	**Supplier**	**Purity (wt%)**	**LogK_{OW}** [16]
Ofloxacin	82419-36-1	361.40	TCI	98.0	1.56
L-menthol	1490-04-6	156.26	Acros Organics	99.5	2.66
Octanoic acid	124-07-2	144.21	Thermo Scientific	98.0	2.7
Decanoic acid	334-48-5	172.26	Thermo Scientific	99.0	3.59
Dodecanoic acid	143-07-7	200.32	Acros Organics	99.0	4.48
1-Decanol	112-30-1	158.28	TCI	98.0	3.47
1-Dodecanol	112-53-8	186.33	Alfa Aesar	98.0	4.36

Table S3. Melting points of the selected HES along with their individual components.

	Name	Molar ratio (HBA:HBD)	Melting point (ºC)	Ref.
Pure compounds	L-Menthol	-	42.6	[17]
	1-Decanol	-	6.9	
	Octanoic acid	-	16.4	
	Decanoic acid	-	31.7	
	Dodecanoic acid	-	44.4	
HES	L-Menthol: Octanoic acid	(1:1)	-4.35	[18]
	L-Menthol: Octanoic acid	(1:2)	2.3	
	L-Menthol: Decanoic acid	(1:1)	13.2	
	L-Menthol: Decanoic acid	(1:2)	20.1	
	L-Menthol: Decanoic acid	(1:3)	24.4	
	Octanoic acid: Decanoic acid	(1:1)	13.84	[19]
	Octanoic acid: Decanoic acid	(2:1)	6.4	
	Decanoic acid: Dodecanoic acid	(2:1)	18.1	[20]
	Decanoic acid: Dodecanoic acid	(3:1)	20.3	
	Octanoic acid: 1-Decanol	(1:1)	-1.3	[21]
	Octanoic acid: 1-Decanol	(2:1)	3.1	
	Decanoic acid: 1-Decanol	(1:1)	14.9	
	Decanoic acid: 1-Decanol	(2:1)	22.4	
	Decanoic acid: 1-Decanol	(3:1)	24.2	

Table S4. Solubility in water of individual components of HES.

HES components	Water solubility (g/100 g water)	Temperature (ºC)	Ref.
L-menthol	0.038	25	[22]
Octanoic acid	0.079	30	
Decanoic acid	0.018	30	[23]
Dodecanoic acid	0.0063	30	
1-Decanol	0.0037	25	[24]
1-Dodecanol	0.0004	25	

Table S5. 2^3 factorial planning.

Run	Coded variables		
	X_1	X_2	X_3
1	-1	-1	-1
2	1	-1	-1
3	-1	1	-1
4	1	1	-1
5	-1	-1	1
6	1	-1	1
7	-1	1	1
8	1	1	1
9	-1.68	0	0
10	1.68	0	0
11	0	-1.68	0
12	0	1.68	0
13	0	0	-1.68
14	0	0	1.68
15	0	0	0
16	0	0	0
17	0	0	0
18	0	0	0
19	0	0	0
20	0	0	0

Table S6. Coded levels of independents variables used in the factorial planning of response surface methodology.

Independent variables	**Axial**	**Factorial**	**Central**	**Factorial**	**Axial**
	-1.682	**-1**	**0**	**1**	**1.682**
X_1 - pH	2.0	2.8	4.0	5.2	6.0
X_2 - OFX concentration(mg/ml)	0.5	0.9	1.5	2.1	2.5
X_3 - ES-water ratio (v/v)	0.6	0.9	1.3	1.8	2.1

Table S7. Predicted logarithm of partition coefficient of OFX (log(K_{OFX})) for the HES in different molar ratios (2:1, 1:1 and 1:2), at 25 ° C using COSMO-RS.

ES	**Molar ratio**		
	1:2	**1:1**	**2:1**
Menthol: C8 acid	2.36	2.04	1.53
Menthol: C10 acid	2.53	2.18	1.66
Menthol: C12 acid	2.61	2.24	1.79
Menthol: C10 alcohol	0.93	0.63	0.60
Menthol: C12 alcohol	0.83	0.43	0.51
C8 acid: C10 acid	2.93	2.58	3.33
C8 acid: C12 acid	3.44	3.04	3.71
C10 acid: C12 acid	3.55	3.23	4.41
C8 acid: C10 alcohol	1.38	1.90	3.17
C8 acid: C12 alcohol	1.34	1.73	2.91
C10 acid: C10 alcohol	1.57	2.16	3.51
C10 acid: C12 alcohol	1.15	1.71	2.36

Table S8. The measured partition coefficient of OFX and extraction efficiency of OFX along with the initial pH of each system for the selected ES at 25 °C.

HES	Molar ratio	pH	Measured K_{OFX}	Error	Measured EE_{OFX} (%)	Error
Menthol: C8 acid	(1:2)	3.98	3.11	0.21	75.64	1.30
Menthol: C10 acid	(1:2)	4.55	6.58	0.31	86.80	0.54
Menthol: C10 acid	(1:3)	4.32	6.38	0.07	86.64	0.35
C8 acid: C10 acid	(2:1)	3.80	3.75	0.22	78.95	0.72
C8 acid: C12 acid	(2:1)	3.92	4.51	0.07	81.83	0.31
C10 acid: C12 acid	(2:1)	4.40	7.35	0.24	88.02	0.35
C10 acid: C12 acid	(3:1)	3.93	5.50	0.04	84.62	0.09
C8 acid: C10 alcohol	(2:1)	4.05	2.77	0.11	73.49	0.77
C10 acid: C10 alcohol	(2:1)	4.60	7.01	0.12	82.87	1.16
C10 acid: C10 alcohol	(3:1)	4.10	4.66	0.33	82.30	1.04

Table S9. Summary of different characteristics and prices of some of the compounds used in LLE of OFX. Prices sourced from official pages of Merck in Portugal (https://www.sigmaaldrich.com/PT/) and Alibaba (https://www.alibaba.com/) as of 19/03/24.

					Merck	**Alibaba**	
Compound	**Solvent Type**	**CAS**	**Melting Point (°C)**	**Boiling Point (°C)**	**Price (€/kg or €/L*)**	**Price ($/kg)**	**Price (€/kg)****
Decanoic acid	Fatty Acid	334-48-5	31.7	268.7	72.0	0.3 - 20.0	0.3 - 17.0
Dodecanoic acid	Fatty Acid	143-07-7	44.3	297.9	52.1	1.0 - 10.0	0.9 - 8.5
Heptanoic acid	Fatty Acid	111-14-8	-10.5	223	147.2	1.0 - 5.0	0.9 – 4.3
Nonanoic acid	Fatty Acid	112-05-0	12.5	255.6	75.3	0.8 - 20.0	0.7 - 17.0
1-ethyl-3-methylimidazolium trifluoromethanesulfonate	Ionic Liquid	145022-44-2		---	1,730.0	50.0 - 220.0	42.5 - 187.0
Thymol	Terpene	89-83-8	47-51	232-234	178.0	1.0- 35.0	0.9 - 29.8
Tetrachloroethane	Volatile Organic	79-34-5	-22.9	146.7	226.0	2.1- 3.5	1.8 – 3.0
L-menthol	Terpene/Alcohol	2216-51-5	42-45		137.0	1.0- 50.0	0.9 - 42.5
Decanol	Alcohol	112-30-1	9.4		64.3	1.0- 10.0	0.9 - 8.5

*Tetrachloroethan; **Assuming exchange rate of 1 US dollar (USD) being equivalent to 0.85 euros (EUR).

Table S10. Experimental data of the partition coefficient and extraction efficiency of OFX obtained through a central composite design, using C10 acid: C12 acid (2:1) HES.

Run	Real variables			OFX extraction efficiency (EE_{OFX}%)
	pH	OFX concentration	HES-water ratio (v/v)	
1	2.8	0.9	0.85	15.43
2	5.2	0.9	0.85	98.06
3	2.8	2.1	0.85	14.19
4	5.2	2.1	0.85	98.10
5	2.8	0.9	1.75	27.01
6	5.2	0.9	1.75	98.74
7	2.8	2.1	1.75	14.27
8	5.2	2.1	1.75	98.83
9	2.0	1.5	1.30	2.94
10	6.0	1.5	1.30	99.25
11	4.0	0.5	1.30	85.22
12	4.0	2.5	1.30	86.81
13	4.0	1.5	0.54	85.85
14	4.0	1.5	2.06	77.18
15	4.0	1.5	1.30	79.06
16	4.0	1.5	1.30	77.80
17	4.0	1.5	1.30	78.91
18	4.0	1.5	1.30	78.85
19	4.0	1.5	1.30	79.20
20	4.0	1.5	1.30	78.33

Table S11. Regression coefficients of the predicted second-order polynomial model for the OFX extraction efficiency obtained from the RSM, $R^2 = 0.94$ and $R_{adj}^2 = 0.89$.

	Regression coefficients	**Standard deviation**	**t-student (10)**	**p-value**
Mean/Interc.	-207.03	3.55	-58.25	<0.0001
(1) pH (L)	100.13	0.98	101.59	<0.0001
pH (Q)	-8.89	0.10	-91.74	<0.0001
(2) C_{OFX} (mg/ml) (L)	-0.45	1.82	-0.25	0.81
C_{OFX} (mg/ml) (Q)	-1.27	0.39	-3.29	0.02
(3) HES-Water ratio (v/v) (L)	43.50	2.51	17.30	<0.0001
HES-Water ratio (v/v) (Q)	-10.12	0.69	-14.68	<0.0001
1L by 2L	2.45	0.26	9.41	<0.0001
1L by 3L	-2.37	0.35	-6.84	<0.0001
2L by 3L	-5.30	0.69	-7.64	<0.0001

Table S12. ANOVA data for the OFX extraction efficiency obtained from the RSM.

	SS	**DF**	**Mean square**	**F**	**p-value**
Regress.	19657.08	9	2184.12	17.98	<0.0001
Residual	1214.58	10	121.46		
Total	20871.66				

Table S13. The simulation parameters for RDF analysis.

Molecule 1	**Molecule 2 (HES)**	**Molar ratio (HBA:HBD)**	**Density (g/cm^3)**	**Molecule1:Molecule2**	**Box size A×B×C ($Å^3$)**
Ofloxacin	L-menthol:C10 acid	(1:2)	0.896	5:100	21.5×21.5×21.5
Ofloxacin	L-menthol:C10 acid	(2:1)	0.896	5:100	21.3×21.3×21.3
Ofloxacin	C8 acid:C10 acid	(2:1)	0.901	5:100	20.9×20.9×20.9
Ofloxacin	C10 acid:C12 acid	(2:1)	0.892	5:100	22.1×22.1×22.1
Ofloxacin	C10 acid:C10 alcohol	(2:1)	0.849	5:100	21.9×21.9×21.9

Figures

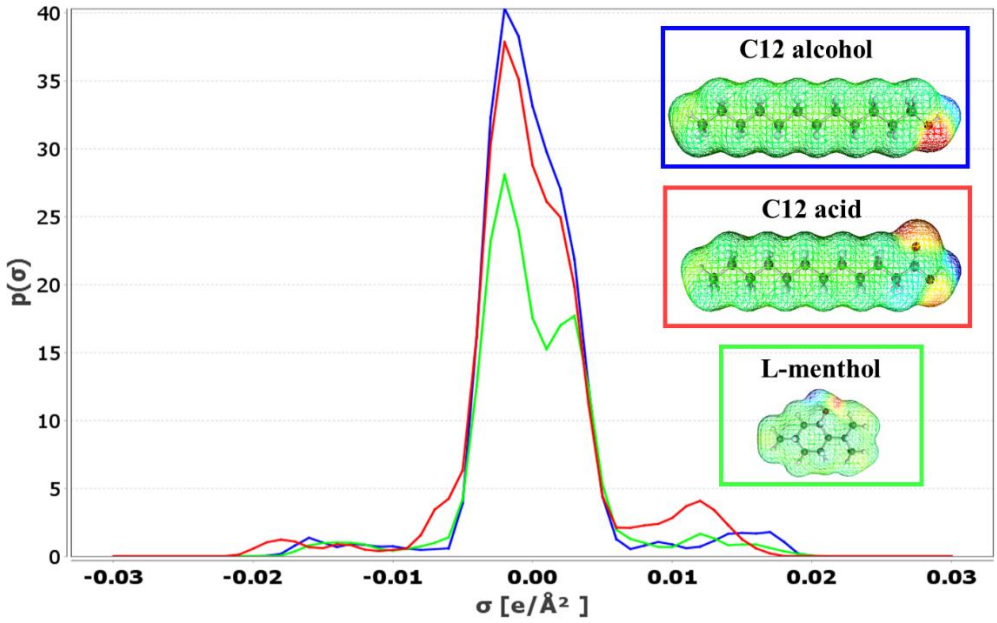

Figure S1. The σ-profiles of the components studied in the HES formation.

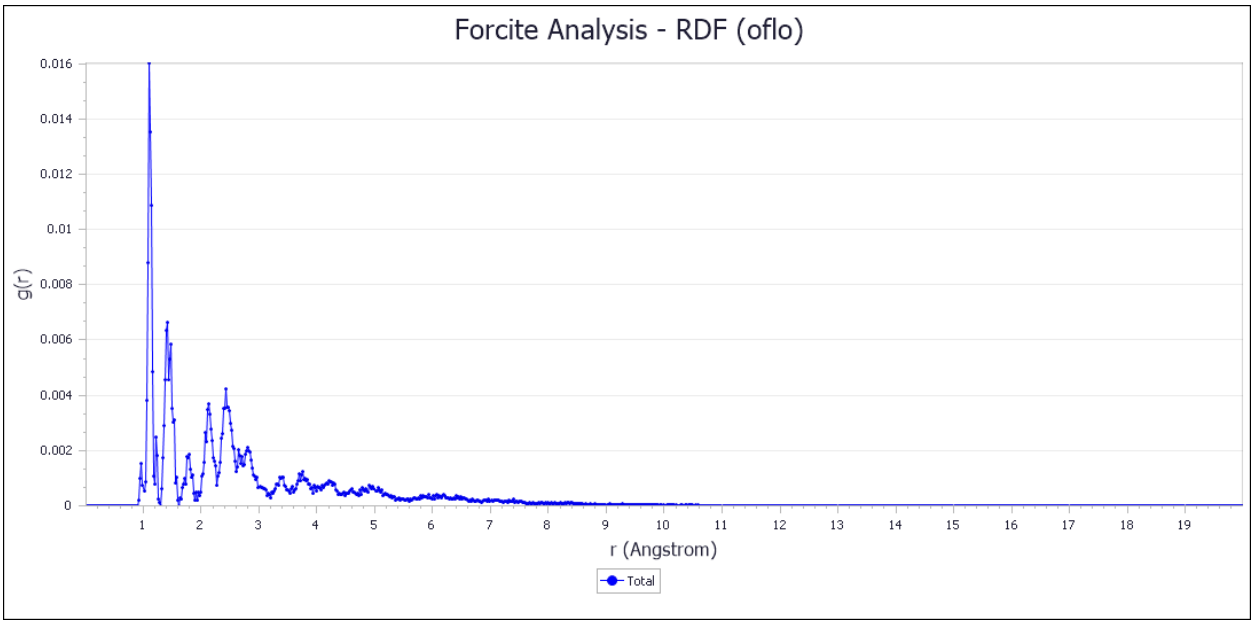

Figure S2. Radial distribution function (RDF) L-menthol:C10 acid (1:2) between the and OFX.

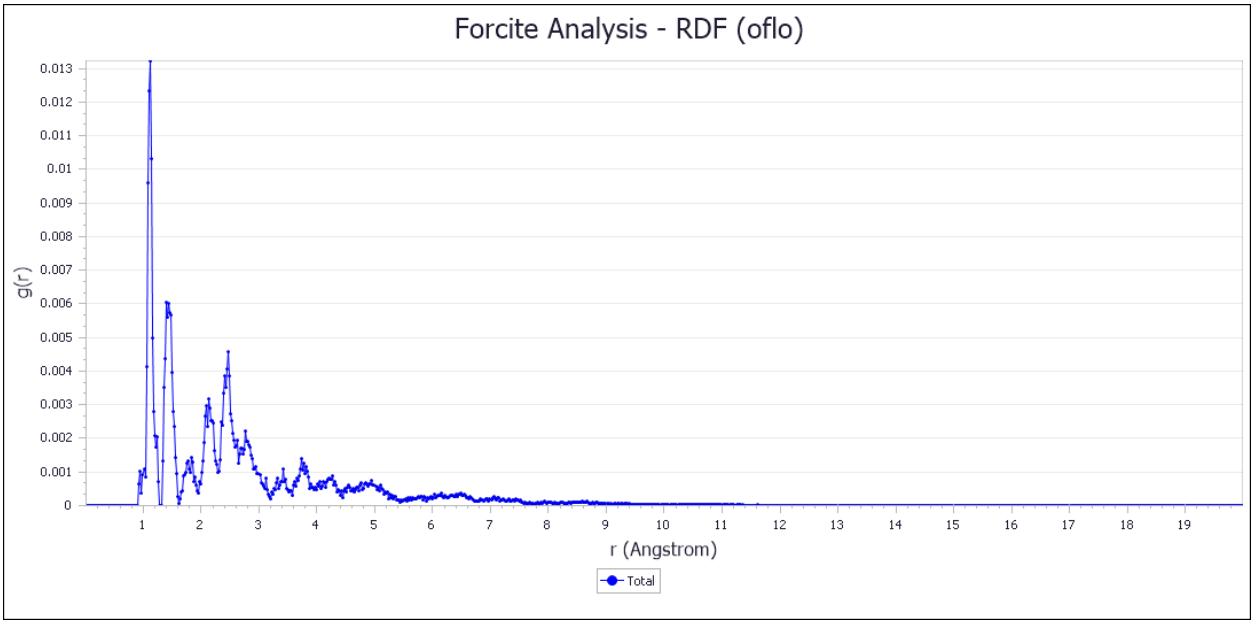

Figure S3. Radial distribution function (RDF) L-menthol:C10 acid (2:1) between the and OFX.

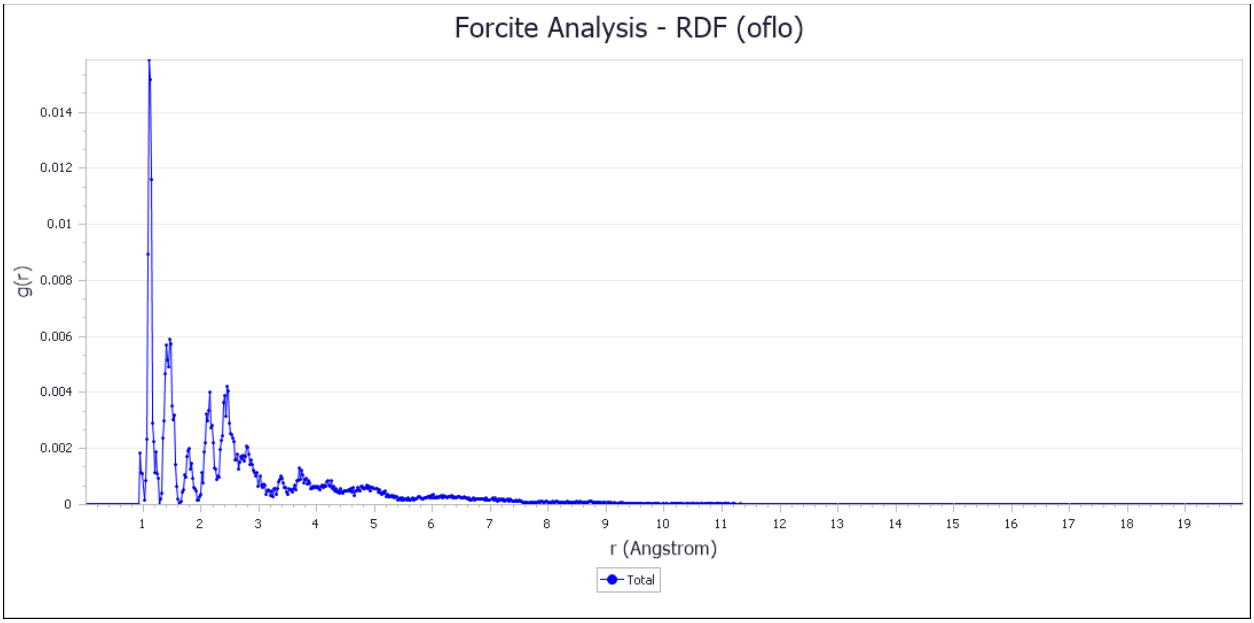

Figure S4. Radial distribution function (RDF) C8 acid:C10 acid (2:1) between the and OFX.

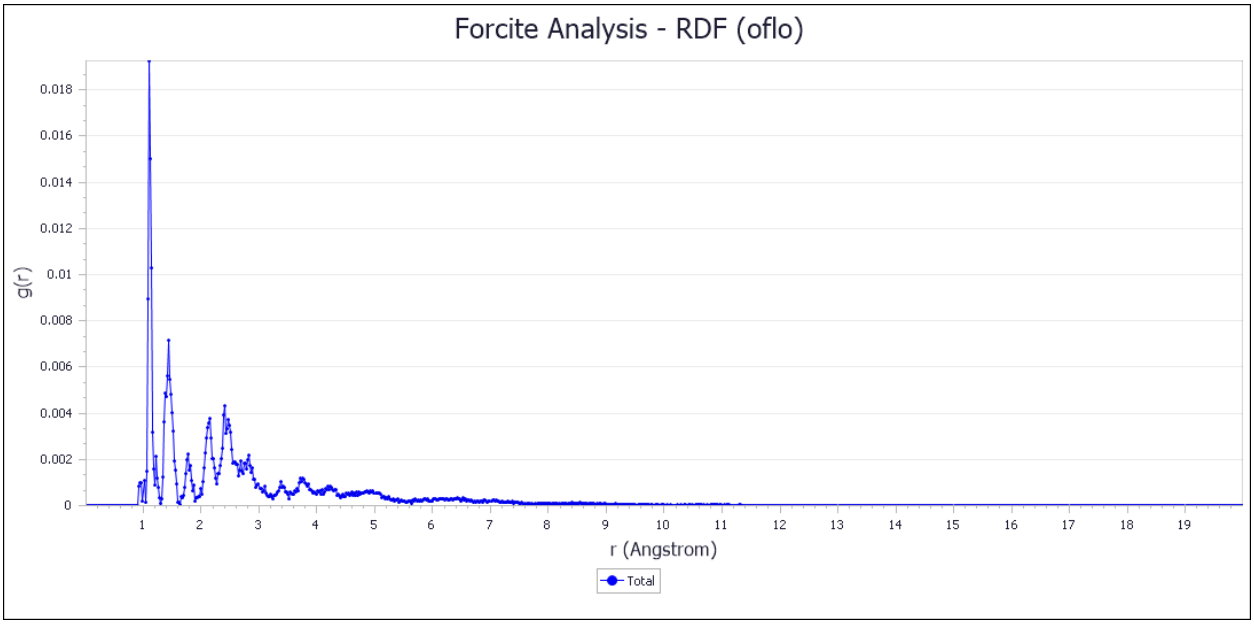

Figure S5. Radial distribution function (RDF) C10 acid:C12 acid (2:1) between the and OFX.

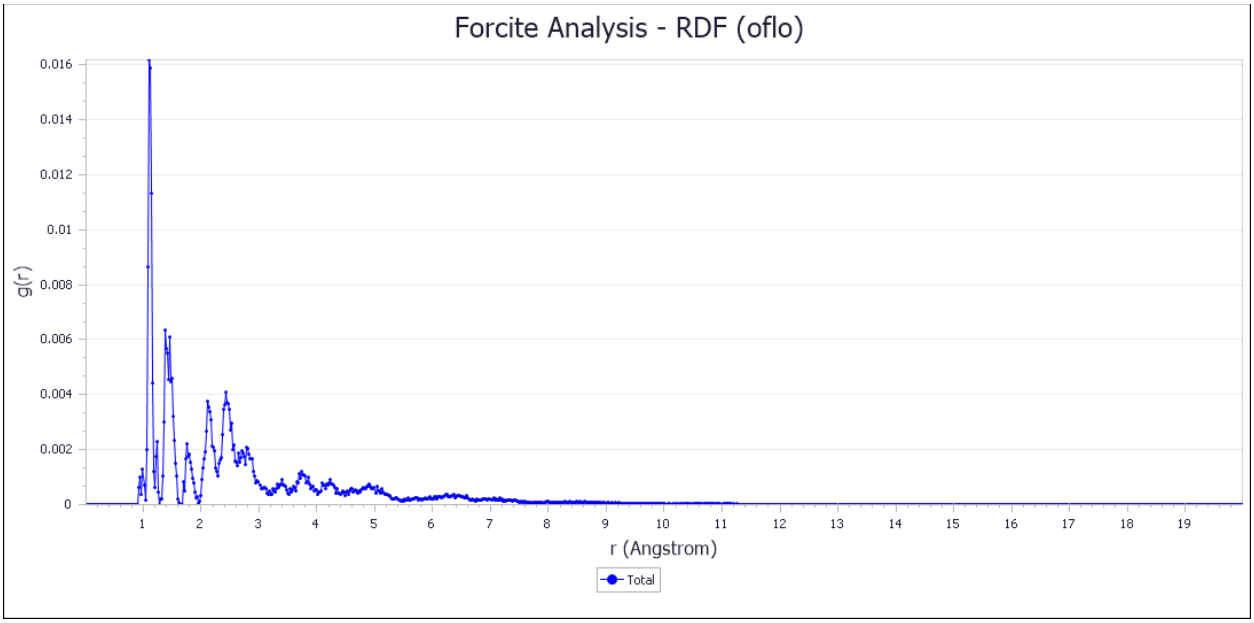

Figure S6. Radial distribution function (RDF) C10 acid:C10 alcohol (2:1) between the and OFX.

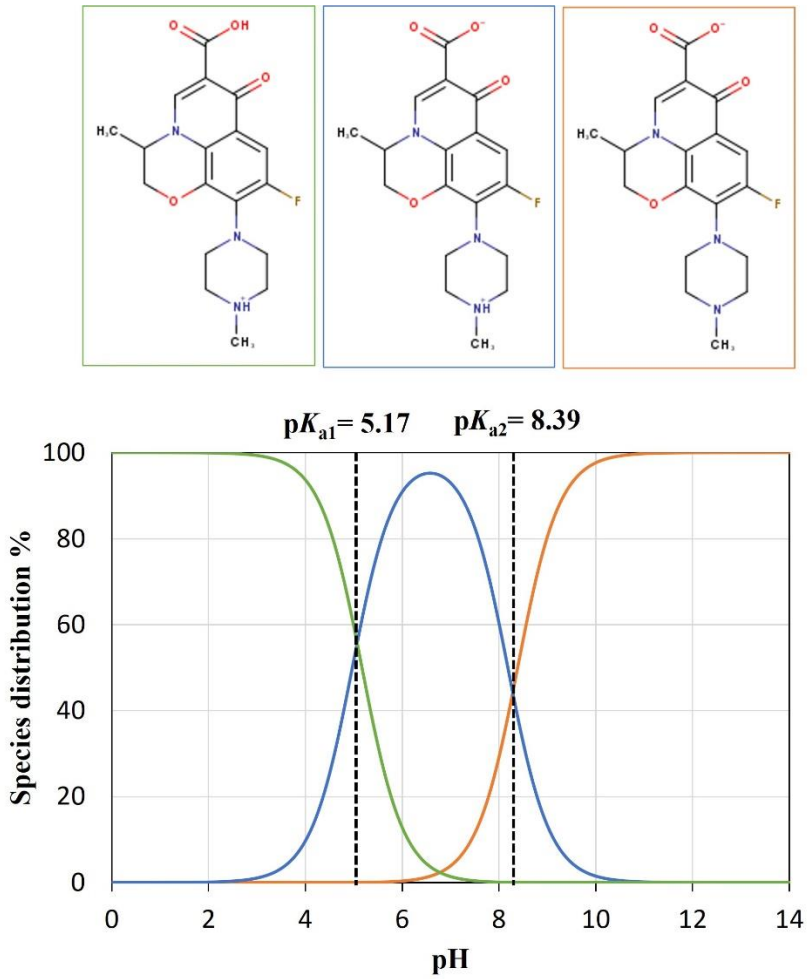

Figure S7. Distribution of distinct forms of OFX at different values of pH [25].

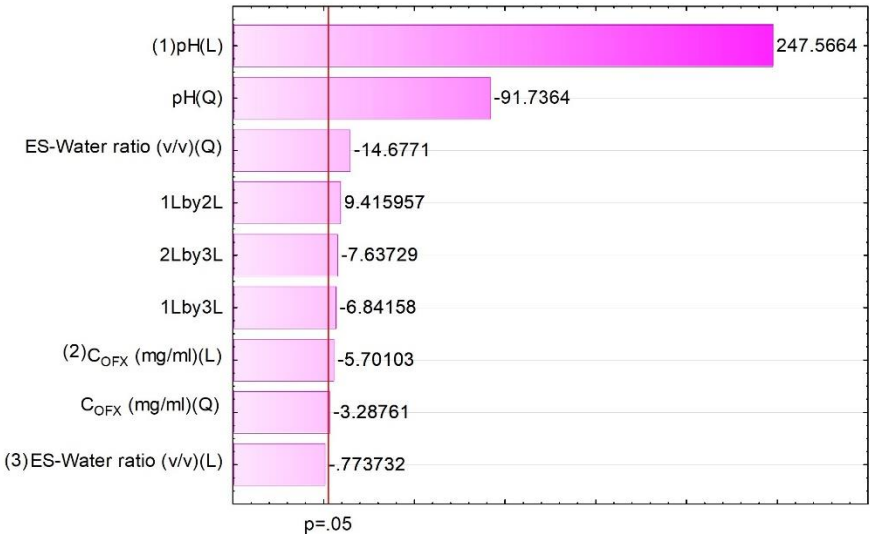

Figure S8. Pareto chart for the standardized main effects in the factor central composite design for the OFX extraction efficiency (EE_{OFX}%), with 95% of confidence.

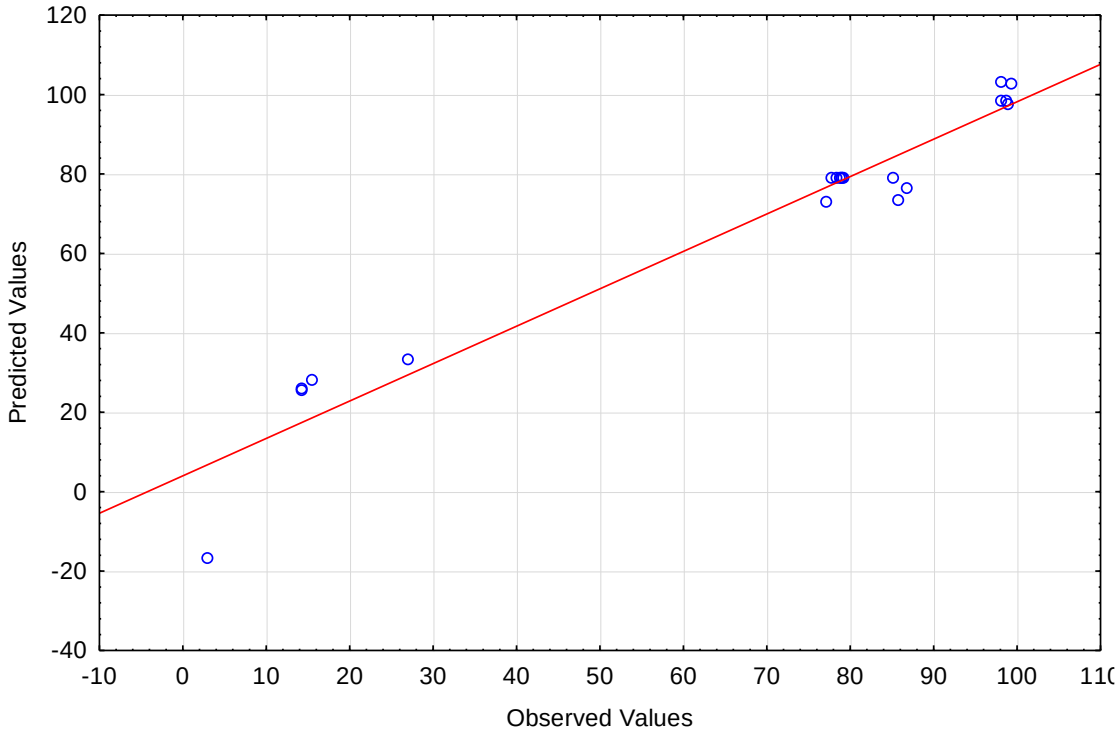

Figure S9. Predict *vs* observed values of the OFX extraction efficiency (EE_{OFX}%) from central composite design.

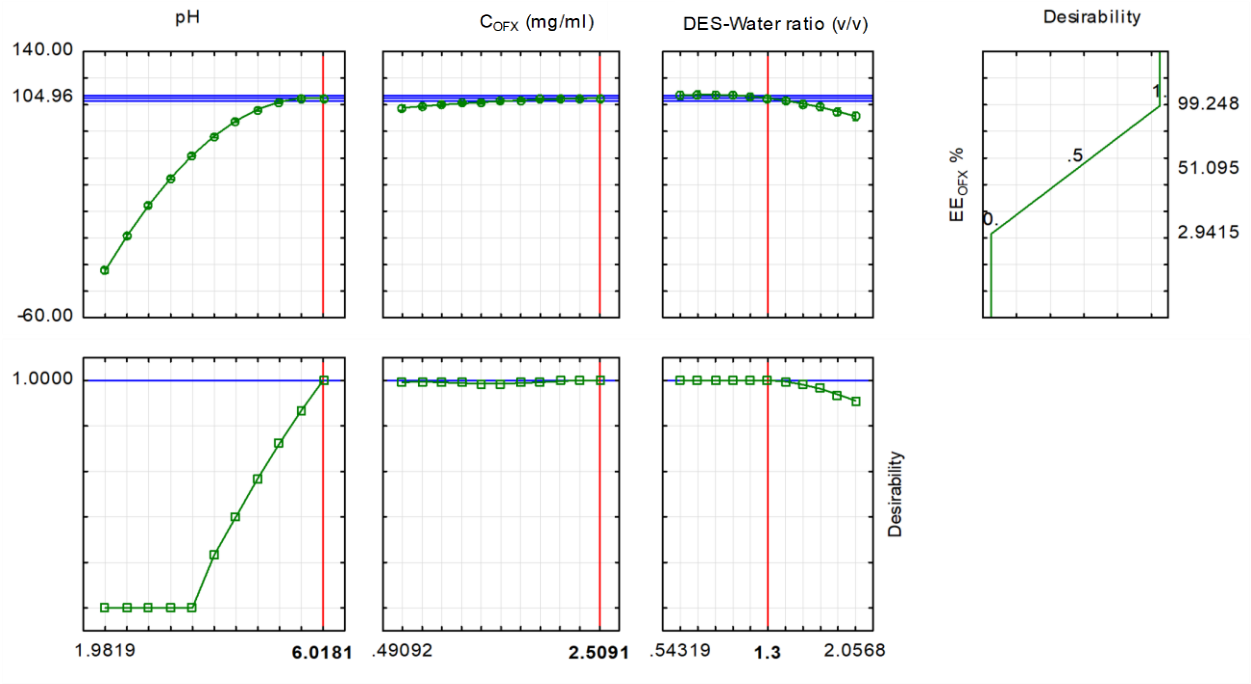

Figure S10. The optimized conditions for maximum partition and extraction of OFX.

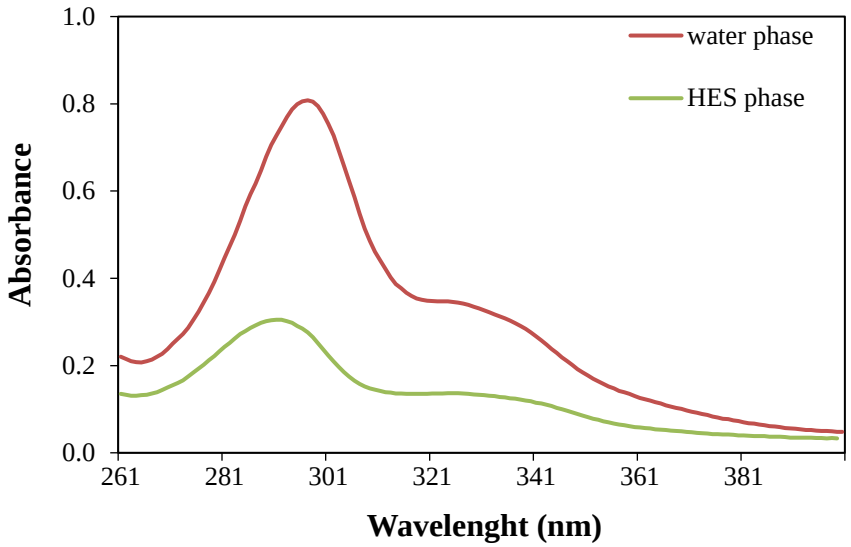

Figure S11. UV-Vis spectra showing the maximum wavelengths of OFX in water and HES phases.

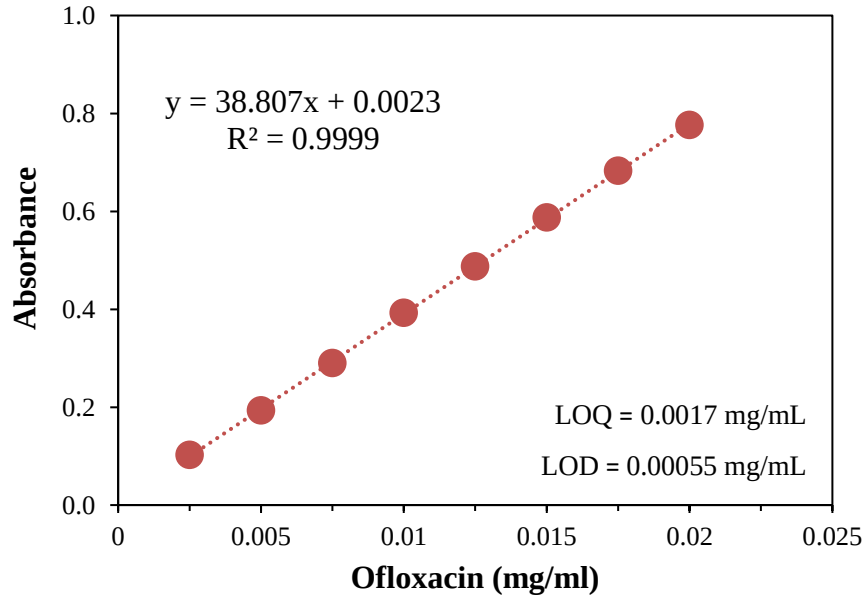

Figure S12. Calibration curve of ofloxacin for HES phase, where LOQ corresponds to the limit of quantification and LOD corresponds to the limit of detection.

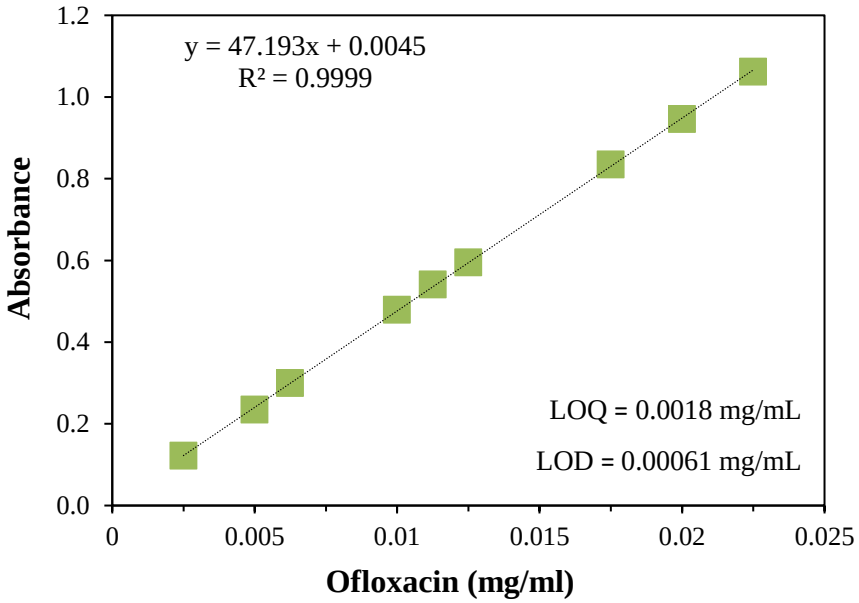

Figure S13. Calibration curve of ofloxacin for HES phase, where LOQ corresponds to the limit of quantification and LOD corresponds to the limit of detection.

Procedures

Liquid-Liquid Extraction (LLE)

The extraction was performed by mixing an equal volume of the HES and an aqueous solution containing OFX at a concentration of 1 mg/ml. The initial mixture was stirred at 50 rpm and (25 ± 1) °C for at least 12 h to promote contact between the two phases. Afterward, the HES was completely separated from the water phase by centrifugation (at 10000 rpm for 10 min in an Eppendorf 5804 centrifuge). In the studied LLE, the top phase corresponds to the HES phase, while the bottom phase is the water phase. After a careful separation of phases, the OFX was quantified in both phases by a UV-spectrophotometry utilizing a SYNERGY|HT microplate reader, BioTek, at a wavelength of 297 nm and 292 nm for HES and water phases (see Figure S11), respectively, using calibration curves (see Figures S12 and S13) previously established. At least three different experiments were performed to determine the average values for partition coefficient and extraction efficiency and their respective standard deviations. In addition, the possible influence of solvents on the quantification method was evaluated using blank control samples.

The radial distribution function (RDF) analysis

The radial distribution function analysis (RDF) for measuring intermolecular interactions was conducted using Material Studio's forcite module, following reported methods from previous studies and Material Studio tutorials [26]. To ensure consistent and accurate results during the simulation, specifying input parameters such as the number of molecules and density is crucial (refer to Table S13 for these data). Moreover, in Material Studio, the choice of forcefield and step length is pivotal, as their sizes influence the duration of computer simulations and the accuracy of performance. In the present analysis, a step length of 1fs and the COMPASS forcefield were selected through extensive trial and error. Following the replication of 3D structures of molecules, geometry optimization was carried out to attain the stable molecular structure. The initial simulation model in the Materials Studio Software was created using the Amorphous Cell module. Initially, the atoms of the model do not evenly share the cubic unit cell. To address this, geometry optimization is performed in the forcite module to minimize the overall energy of the simulation box. Employing three-dimensional periodic boundary

conditions, the cell utilizes the Ewald electrostatic summation method [26]. Energy minimization is carried out using the smart minimization method. Subsequently, under the NVT ensemble (a simulation protocol where the number of atoms (N), volume (V), and temperature (T) are assumed to be constant), a 200 ps Molecular Dynamics (MD) run is conducted to achieve appropriate cell equilibration [26]. To produce a more realistic model, the amorphous cell or simulation model undergoes annealing. A time step of 1fs is chosen to prevent overlap of molecules within the box. To maintain a constant pressure of 1 atm and attain equilibrium density, The simulation box includes 100 molecules of each HES and 5 molecules of ofloxacin.

References

[1] H. Sereshti, F. Karami, N. Nouri, A green dispersive liquid-liquid microextraction based on deep eutectic solvents doped with β-cyclodextrin: Application for determination of tetracyclines in water samples, Microchemical Journal 163 (2021) 105914. https://doi.org/10.1016/J.MICROC.2020.105914.

[2] W. Ma, K.H. Row, pH-induced deep eutectic solvents based homogeneous liquid-liquid microextraction for the extraction of two antibiotics from environmental water, Microchemical Journal 160 (2021) 105642. https://doi.org/10.1016/j.microc.2020.105642.

[3] L. Qiao, R. Sun, C. Yu, Y. Tao, Y. Yan, Novel hydrophobic deep eutectic solvents for ultrasound-assisted dispersive liquid-liquid microextraction of trace non-steroidal anti-inflammatory drugs in water and milk samples, Microchemical Journal 170 (2021) 106686. https://doi.org/10.1016/J.MICROC.2021.106686.

[4] K. Li, Y. Jin, D. Jung, K. Park, H. Kim, J. Lee, In situ formation of thymol-based hydrophobic deep eutectic solvents: Application to antibiotics analysis in surface water based on liquid-liquid microextraction followed by liquid chromatography, J Chromatogr A 1614 (2020) 460730. https://doi.org/10.1016/j.chroma.2019.460730.

[5] F. Shakirova, A. Shishov, A. Bulatov, Automated liquid-liquid microextraction and determination of sulfonamides in urine samples based on Schiff bases formation in natural deep eutectic solvent media, Talanta 234 (2021) 122660. https://doi.org/10.1016/J.TALANTA.2021.122660.

[6] A.Y. Shishov, M. V. Chislov, D. V. Nechaeva, L.N. Moskvin, A. V. Bulatov, A new approach for microextraction of non-steroidal anti-inflammatory drugs from human urine

samples based on in-situ deep eutectic mixture formation, J Mol Liq 272 (2018) 738–745. https://doi.org/10.1016/J.MOLLIQ.2018.10.006.

[7] Y. Liu, W. Xu, H. Zhang, W. Xu, Hydrophobic deep eutectic solvent-based dispersive liquid–liquid microextraction for the simultaneous enantiomeric analysis of five β-agonists in the environmental samples, Electrophoresis 40 (2019) 2828–2836. https://doi.org/10.1002/ELPS.201900149.

[8] C. Florindo, F. Lima, L.C. Branco, I.M. Marrucho, Hydrophobic Deep Eutectic Solvents: A Circular Approach to Purify Water Contaminated with Ciprofloxacin, ACS Sustain Chem Eng 7 (2019) 14739–14746. https://doi.org/10.1021/acssuschemeng.9b02658.

[9] X. Di, X. Zhao, X. Guo, Hydrophobic deep eutectic solvent as a green extractant for high-performance liquid chromatographic determination of tetracyclines in water samples, J Sep Sci 43 (2020) 3129–3135. https://doi.org/10.1002/JSSC.202000477.

[10] H. Sereshti, G. Abdolhosseini, S. Soltani, F. Jamshidi, N. Nouri, Natural thymol-based ternary deep eutectic solvents: Application in air-bubble assisted-dispersive liquid-liquid microextraction for the analysis of tetracyclines in water, J Sep Sci 44 (2021) 3626–3635. https://doi.org/10.1002/JSSC.202100495.

[11] W. Tang, Y. Dai, K.H. Row, Evaluation of fatty acid/alcohol-based hydrophobic deep eutectic solvents as media for extracting antibiotics from environmental water, Anal Bioanal Chem 410 (2018) 7325–7336. https://doi.org/10.1007/s00216-018-1346-6.

[12] Q. Qu, Y. Lv, L. Liu, K.H. Row, T. Zhu, Synthesis and characterization of deep eutectic solvents (five hydrophilic and three hydrophobic), and hydrophobic application for microextraction of environmental water samples, Anal Bioanal Chem 411 (2019) 7489–7498. https://doi.org/10.1007/s00216-019-02143-z.

[13] A.G. Pekel, E. Kurtulbaş, İ. Toprakçı, S. Şahin, Menthol-based deep eutectic solvent for the separation of carbamazepine: reactive liquid-liquid extraction, Biomass Convers Biorefin 12 (2022) 1249–1256. https://doi.org/10.1007/S13399-020-00707-Z.

[14] E. Kurtulbaş, A.G. Pekel, İ. Toprakçı, G. Özçelik, M. Bilgin, S. Şahin, Hydrophobic carboxylic acid based deep eutectic solvent for the removal of diclofenac, Biomass Convers Biorefin 12 (2022) 2219–2227. https://doi.org/10.1007/S13399-020-00721-1.

[15] L. Chen, L. Ge, Q. Liang, Z. Zhao, K. Yang, Eutectic solvents formed by (+)-DTTA and L-menthol as novel chiral recognition and separation media for enantioselective extraction

of valsartan enantiomers, J Mol Liq 368 (2022) 120818. https://doi.org/10.1016/J.MOLLIQ.2022.120818.

[16] ChemSpider, http://www.chemspider.com/ (accessed June 30, 2022).

[17] G. Teixeira, D.O. Abranches, O. Ferreira, J.A.P. Coutinho, Estimating the Melting Temperatures of Type V Deep Eutectic Solvents, Ind Eng Chem Res 62 (2023) 14638–14647. https://doi.org/10.1021/acs.iecr.3c01063.

[18] M.A.R. Martins, E.A. Crespo, P.V.A. Pontes, L.P. Silva, M. Bülow, G.J. Maximo, E.A.C. Batista, C. Held, S.P. Pinho, J.A.P. Coutinho, Tunable Hydrophobic Eutectic Solvents Based on Terpenes and Monocarboxylic Acids, ACS Sustain Chem Eng 6 (2018) 8836–8846. https://doi.org/10.1021/ACSSUSCHEMENG.8B01203.

[19] M.C. Costa, M. Sardo, M.P. Rolemberg, J.A.P. Coutinho, A.J.A. Meirelles, P. Ribeiro-Claro, M.A. Krähenbühl, The solid–liquid phase diagrams of binary mixtures of consecutive, even saturated fatty acids, Chem Phys Lipids 160 (2009) 85–97. https://doi.org/10.1016/J.CHEMPHYSLIP.2009.05.004.

[20] C. Florindo, L. Romero, I. Rintoul, L.C. Branco, I.M. Marrucho, From Phase Change Materials to Green Solvents: Hydrophobic Low Viscous Fatty Acid-Based Deep Eutectic Solvents, ACS Sustain Chem Eng 6 (2018) 3888–3895. https://doi.org/10.1021/acssuschemeng.7b04235.

[21] N.D.D. Carareto, T. Castagnaro, M.C. Costa, A.J.A. Meirelles, The binary (solid + liquid) phase diagrams of (caprylic or capric acid) + (1-octanol or 1-decanol), J Chem Thermodyn 78 (2014) 99–108. https://doi.org/10.1016/J.JCT.2014.06.011.

[22] S.M. Vilas-Boas, M.C. da Costa, J.A.P. Coutinho, O. Ferreira, S.P. Pinho, Octanol-Water Partition Coefficients and Aqueous Solubility Data of Monoterpenoids: Experimental, Modeling, and Environmental Distribution, Ind Eng Chem Res 61 (2022) 3154–3167. https://doi.org/10.1021/ACS.IECR.1C04196.

[23] K. Bober, M. Garus, RP-HPTLC Application in the Investigation of Solubility in Water of Long-Chain Fatty Acids, J Liq Chromatogr Relat Technol 29 (2006) 2787–2794. https://doi.org/10.1080/10826070601001476.

[24] C.L. Yaws, J.R. Hopper, S.D. Sheth, M. Han, R.W. Pike, Solubility and henry's law constant for alcohols in water, Waste Management 17 (1998) 541–547. https://doi.org/10.1016/S0956-053X(97)10057-5.

[25] ChemAxon, MarvinSketch 22.13, (2022). http://www.chemaxon.com (accessed March 20, 2023).

[26] M. Sharif, X. Wu, Y. Yu, T. Zhang, Z. Zhang, Estimation of diffusivity and intermolecular interaction strength of secondary and tertiary amine for CO2 absorption process by molecular dynamic simulation, Mol Simul 48 (2022) 484–494. https://doi.org/10.1080/08927022.2022.2027406.